

**Highlights of this chapter:** This chapter methods to fabricate artificial nanostructures are introduced. Epitaxy as well as lithography is discussed.

## 5 Fabrication Tools

### 5.1 Introduction

For the fabrication principles in nanotechnology, one distinguishes between so-called top-down and bottom-up approaches. Top-down approaches seek to create nanoscale devices by using larger, externally-controlled tools to direct their assembly. Here, often traditional workshop or microfabrication methods are used to cut, mill, and shape materials into the desired shape and order. Micropatterning techniques, such as photolithography and inkjet printing belong to this category. Bottom-up approaches, in contrast, seek to have smaller (usually molecular) components built up into more complex assemblies. These techniques use the chemical properties of single molecules to cause single-molecule components to (a) self-organize or self-assemble into some useful conformation, or (b) rely on positional assembly. These approaches utilize the concepts of molecular self-assembly and/or molecular recognition.

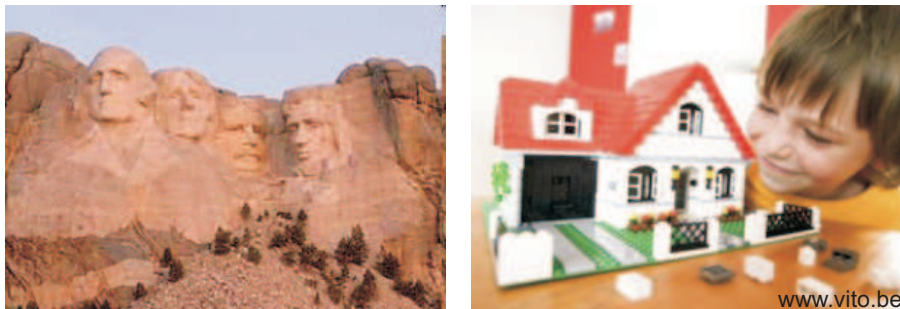


Figure 125: Top-down vs. bottom-up technologies.

### 5.2 Epitaxy

Epitaxial techniques are today the mostly utilized techniques to create solid-state nano-scaled devices. The term *epitaxy* comes from a Greek root (*epi* “above” and *taxis* “in ordered manner”) and refers to the method of depositing a mono-crystalline film on a mono-crystalline substrate. The deposited film is denoted as epitaxial film or epitaxial layer.

Epitaxial films may be grown from gaseous or liquid precursors. Because the substrate acts as a seed crystal, the deposited film takes on a lattice structure and orientation identical to those of the substrate. This is different from other thin-film deposition methods which deposit poly-crystalline or amorphous films, even on single-crystal substrates. If a film is deposited on a substrate of the same composition, the process is called homo-epitaxy; otherwise it is called hetero-epitaxy. The latter, is often applied to growing crystalline films of materials of which single crystals cannot be obtained and to fabricating integrated crystalline layers of different materials, such as quantum dots.

Here we discuss two major epitaxial techniques, Molecular Beam Epitaxy (MBE) and Metal-Organic Chemical Vapour Deposition (MOCVD).

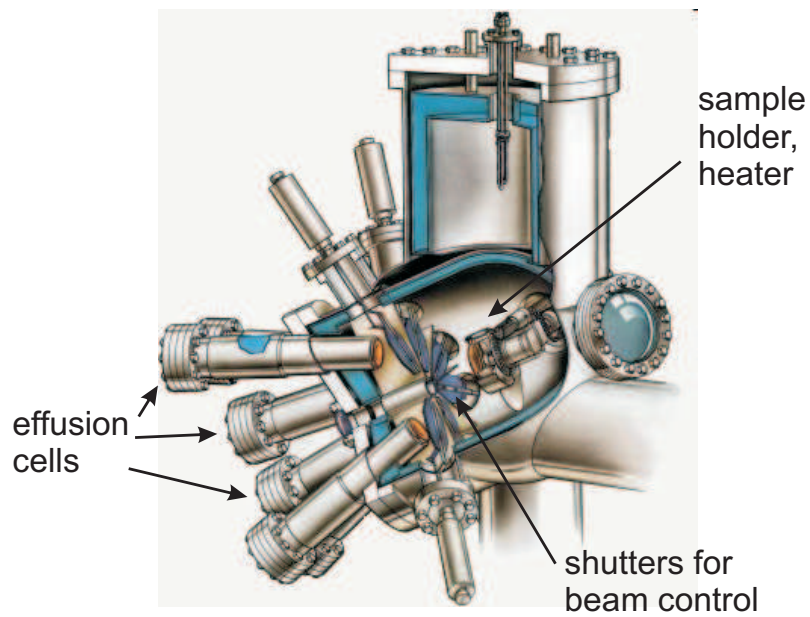
### 5.2.1 Molecular Beam Epitaxy

Molecular Beam Epitaxy (MBE) was invented in the late 1960s at Bell Telephone Laboratories by J. R. Arthur and Alfred Y. Cho.

The growth process takes place in an ultra-high vacuum environment ( $< 10^{-9}$  mbar), such that the mean free path of the particles is larger than the geometrical size of the chamber. The term "beam" means that evaporated atoms do not interact with each other or with vacuum chamber gases until they reach the wafer. Figure 126 shows a typical MBE chamber.

Ultra-pure elements such as gallium and arsenic are heated in separate effusion cells until they begin to slowly sublime from the solid or evaporate from the liquid phase. The effusion cell temperature is typically used to control the flux of the atomic beam. For some molecules/atoms (e.g. nitrogen), gas cells are used as well. The composition of the different materials is controlled, using mechanical shutters in front of the output ports of the cells.

The gaseous elements then condense on the substrate, where they may react with each other. In order to obtain a high mobility of the adatoms, the substrate is heated to high temperatures (typ.  $\approx 300^\circ$  C for II-VI materials, such as ZnSe, and  $\approx 600^\circ$  C for III-V materials, such as GaAs). In order to maintain the crystal structure, the substrates have to be mono-crystalline wafers with carefully cleaned surfaces.



[www.hlphys.jku.at/fkphys/epitaxy/mbe.html](http://www.hlphys.jku.at/fkphys/epitaxy/mbe.html)

Figure 126: Schematics of an MBE chamber.

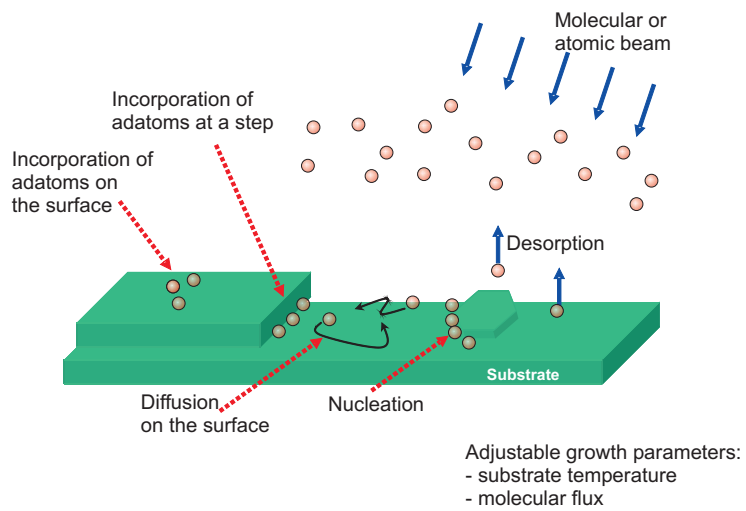


Figure 127: Different processes during the MBE growth.

Figure 127 shows the different processes which the adatoms undergo during growth. Nucleation of atoms can take place on mono-atomic steps, on defects, or directly on the surface. The nucleation process is in competition with sublimation of atoms from the surface, depending on the substrate temperature and the molecular beam flux.

During operation, RHEED (Reflection High Energy Electron Diffraction) is often used for monitoring the growth of the crystal layers. This technique uses an electron beam with energies of some ten keV. The electrons are accelerated in an electron gun and are focussed with a shallow angle on the sample surface. Incident electrons diffract from atoms at the surface of the sample, and a small fraction of the diffracted electrons interfere constructively at specific angles and form regular patterns on the detector. The diffraction pattern is monitored on a fluorescing screen.

The diffraction pattern provides various information about the surface structure, as the penetration depth of the electrons is only few monolayers. Figure 128 (top) compares the pattern of a flat surface (stripes) with that of a roughened surface, e.g. due to quantum dot formation (spots). The number of stripes/spots indicates the crystal structure of the surface (so-called surface reconstruction), while the distance between neighbouring stripes is inverse proportional to the lattice constant at the surface. Finally, the intensity variation of the stripes allows a direct counting of the number of deposited monolayers (figure 128, bottom). Here one makes use of the fact, that at a semi-finished monolayer, increased scattering of the electrons appears and consequently the intensity of the directly reflected e-beam is reduced. Monitoring these RHEED oscillations allows to track the material deposition with sub-monolayer accuracy.

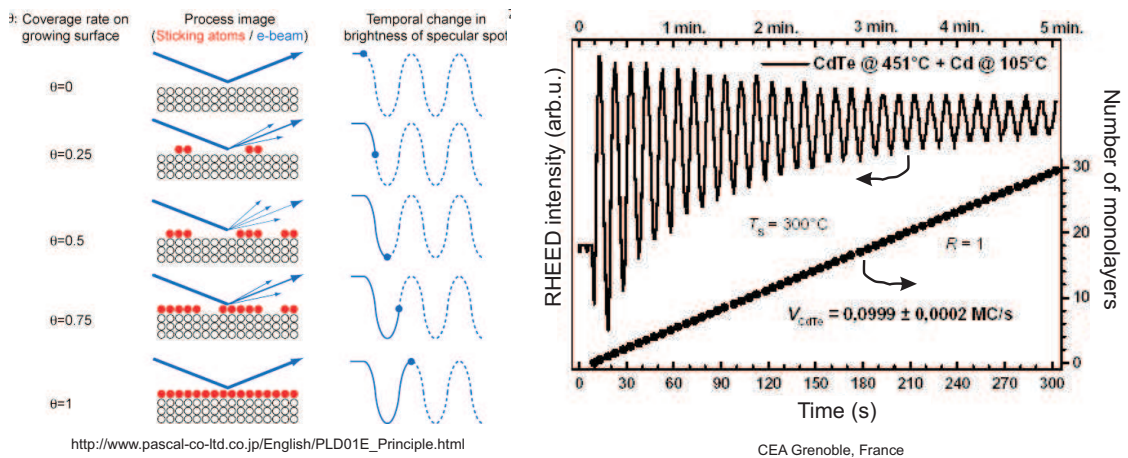
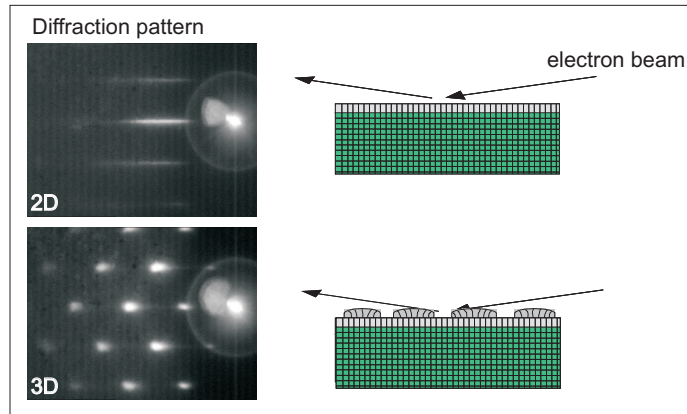
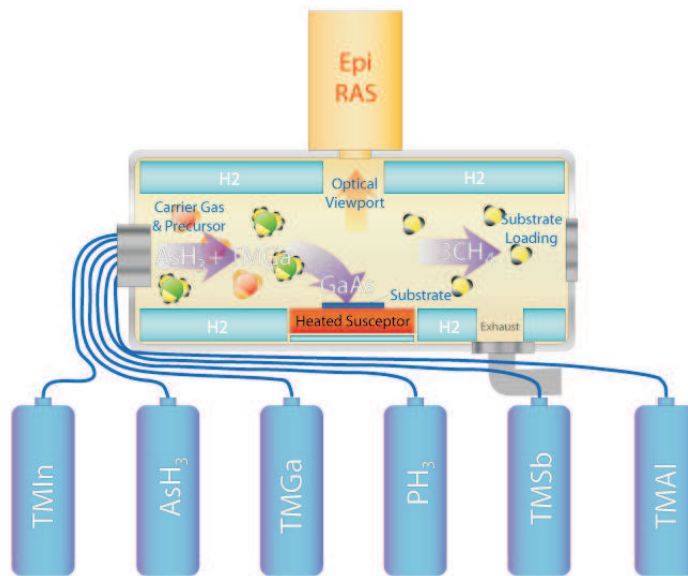


Figure 128: Top: RHEED patterns for a flat/2D surface and a structured/3D surface. Bottom left: principle of RHEED oscillations. Bottom right: experimental RHEED oscillations and number of monolayers for CdTe growth.

### 5.2.2 Metal-Organic Chemical Vapour Deposition

Metal-Organic Chemical Vapour Deposition (MOCVD), also known as Metal-Organic Vapour Phase Epitaxy (MOVPE), is a chemical vapour deposition method of epitaxial growth of materials, especially compound semiconductors from the surface reaction of organic compounds or metalorganics and metal hydrides containing the required chemical elements. In contrast to MBE, the growth of crystals is by chemical reaction instead of physical deposition. This takes place not in a vacuum, but from the gas phase at moderate pressures (2 to 100 kPa).



[http://www.photonics.ethz.ch/research/core\\_competences/technology/epitaxial\\_growth/movpe](http://www.photonics.ethz.ch/research/core_competences/technology/epitaxial_growth/movpe)

Figure 129: Schematics of MOCVD growth.

The principle of MOCVD on the example of a GaAs film is the following: gaseous compounds of gallium or arsenic are needed as so-called precursors. For As, the arsenic hydride ( $\text{AsH}_3$ ) and for Ga a metal-organic compound such as trimethyl gallium (TMGa) is mainly used, respectively. They are fed into the reactor with the aid of a carrier gas (hydrogen or nitrogen). The reactor contains the substrate (GaAs wafer) which is heated. The temperatures range from about 500 to 1500° C depending on the material system to be produced. For pure GaAs the chemical bounds of the compounds have to be broken. This already occurs partially in the gas phase due to the heat emitted from the substrate or by collisions with the molecules

of the carrier gas. The fragments move to the substrate surface, together with undamaged arsine and TMGa, where they settle and migrate over the wafer. Due to the high temperature and the reactions accelerated by the substrate, additional bonds are split up so that ultimately pure gallium or arsenic can be deposited. In this way, a new GaAs layer grows on the wafer monolayer by monolayer. The remainder of the starting molecules, the methyl groups of TMGa and the hydrogen of arsine, partially combine forming methane. Together with molecules which have not reacted they detach from the surface and are flushed out of the reactor by the carrier gas stream.

The advantage of MOCVD over MBE is the much increased growth speed up to 1 nm/s, which makes this technique ideal for mass production. Due to the absence of high-vacuum components, MOCVD is comparably inexpensive and easy to maintain. The main expenses are the high-purity precursors and (compared to MBE) the low material efficiency. The main disadvantage of MOCVD compared to MBE is, that MOCVD utilizes elemental compounds. So a comparably large amount of impurities (such as hydrogen, nitrogen, or oxygen) are implanted into the crystal.

### 5.3 Epitaxial Growth of Heterostructures

A heterostructure is the interface that occurs between two layers or regions of different crystalline semiconductors. These semiconducting materials have in general unequal band gaps. Heterostructures allow *band-gap engineering* which is used to make and optimize the electronic energy bands in many solid state device applications, such as semiconductor lasers, solar cells and transistors to name a few.

#### 5.3.1 Quantum confinement in heterostructures

In heterostructures of very small spatial dimensions, the motion of charge carriers is restricted. They are forced into a quantum confinement regime, leading to formation of a set of discrete energy levels. In this way arbitrary potentials can be created for electrons and holes in a heterostructure.

The following figure 130 shows a type-I structure with confinement for both electrons and holes.

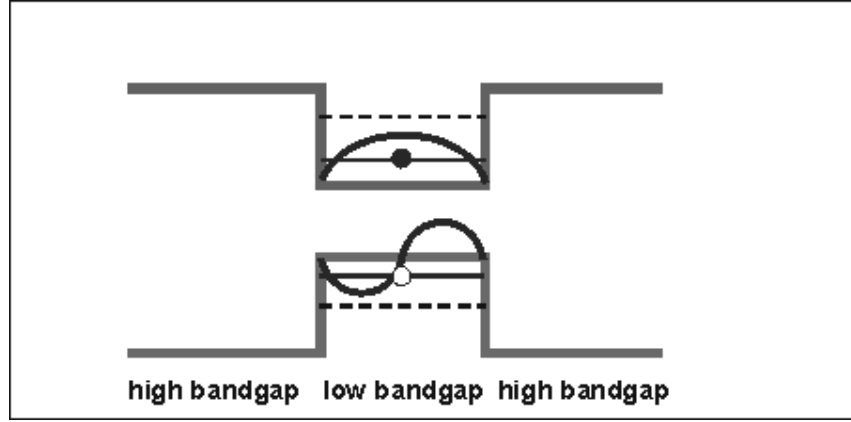


Figure 130: Schematics of a type-I heterostructure and pictorial image of the electron hole wave-functions.

A simple theoretical description of confinement in a heterostructure (in one dimension) starts with assuming the following potential:

$$V(z) = 0 \quad \text{for } (-L/2) < z < (L/2) \quad (\text{region A}) \quad (262)$$

$$V(z) = V_0 \quad \text{for } z < (-L/2) \text{ or } z > (L/2) \quad (\text{region B}) \quad (263)$$

An appropriate ansatz for the (electronic) wavefunction is:

$$\Psi(r) = N^{-1/2} \sum_i C_{nA}(R_i) a_{nA}(r - R_i) \quad \text{for } (-L/2) < z < (L/2) \quad (264)$$

$$\Psi(r) = N^{-1/2} \sum_i C_{nB}(R_i) a_{nB}(r - R_i) \quad \text{for } z < (-L/2) \text{ or } z > (L/2) \quad (265)$$

Here,  $a_{nA}$  and  $a_{nB}$  are Wannier functions which depend only on  $(r - R_i)$  with  $R_i$  being a lattice vector. In case of strong localization one can imagine the Wannier functions as analogues of atomic orbitals. The coefficients  $C_{nA}$  and  $C_{nB}$  are the envelope functions.

By plugging this ansatz into the Schrödinger equation one finds for a specific band  $n$ :

$$\left[ - \left( \frac{\hbar^2}{2m_A^*} \right) \frac{\partial^2}{\partial R^2} \right] C_A(R) \approx E C_A(R) \quad (266)$$

for  $(-L/2) < z < (L/2)$

and

$$\left[ - \left( \frac{\hbar^2}{2m_B^*} \right) \frac{\partial^2}{\partial R^2} + V_0(z) \right] C_B(R) \approx E C_B(R) \quad (267)$$

for  $z < (-L/2)$  or  $z > (L/2)$  with the effective masses  $m_A^*$  and  $m_B^*$ .

As  $V_0$  depends only on  $z$  it is possible to factorize the solution:

$$C_{A,B} = \Phi_{A,B}(x, y) \Psi_{A,B}(z) \quad (268)$$

In  $x, y$ -direction one finds the solution for a free particle:

$$\Phi_{A,B}(x, y) \propto \exp[\pm i(k_x x + k_y y)] \quad (269)$$

Here  $k_x$  and  $k_y$  are equal for both regions  $A$  and  $B$ .

For the functions  $\Psi_A(z)$  and  $\Psi_B(z)$  it is:

$$-\left(\frac{\hbar^2}{2m_A^*}\right) \left[ \frac{\partial^2}{\partial z^2} + k_x^2 + k_y^2 \right] \Psi_A(z) \approx E \Psi_A(z) \quad (270)$$

for  $(-L/2) < z < (L/2)$

and

$$\left[ -\left(\frac{\hbar^2}{2m_B^*}\right) \left( \frac{\partial^2}{\partial z^2} + k_x^2 + k_y^2 \right) + V_0 \right] \Psi_B(z) \approx E \Psi_B(z) \quad (271)$$

for  $z < (-L/2)$  oder  $z > (L/2)$

For the case of  $k_x = k_y = 0$  these equations describe the problem of a particle in a one dimensional potential well.

For the case

$$E - \left(\frac{\hbar^2}{2m_B^*}\right) (k_x^2 + k_y^2) < V_0 \quad (272)$$

there are exponentially decreasing solutions outside the potential well (region  $B$ ) of the form

$$\Psi_B(z) = \alpha_1 e^{\tau z} \quad \text{for } z < (-L/2) \quad (273)$$

$$\Psi_B(z) = \alpha_2 e^{-\tau z} \quad \text{for } z > (L/2) \quad (274)$$

Within the potential well (region  $A$ ) there is

$$\Psi_A(z) = \beta_1 \cos(k_z) \quad \text{for } z < (-L/2) \quad (275)$$

$$\Psi_A(z) = \beta_2 \sin(k_z) \quad \text{for } z > (L/2) \quad (276)$$

with appropriate decay constants  $\tau$  and wave vectors  $k_z$ , respectively.

The continuity of the functions at the boundary and normalization determines  $\alpha_1, \alpha_2, \beta_1, \beta_2$ .

There are analytic expression for the allowed eigenvectors  $E_n(k_x, k_y)$  in the limiting case  $V_0 \rightarrow \infty$ :

$$E_n(k_x, k_y) = \left( \frac{\hbar^2}{2m_A^*} \right) \left[ \left( \frac{n\pi}{L} \right)^2 + k_x^2 + k_y^2 \right] \quad n = 1, 2, 3 \dots \quad (277)$$

The following figure 131 shows the eigenvalues schematically:

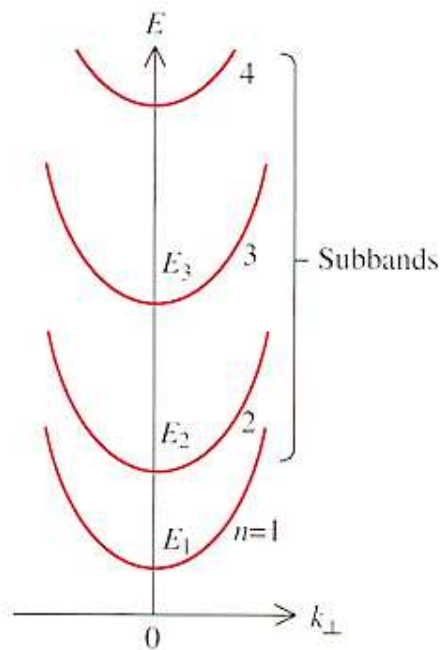


Figure 131: Schematic representation of the energy eigenvalues of a quantum film. [from Yu & Cardona, "Fundamentals of Semiconductors"]

A similar analysis holds also for the wavefunctions of the holes.

Obviously, the description can be generalized for the case of 'confinement' in more than one dimension. One subdivides:

- confinement in one dimension: **quantum films**
- confinement in two dimensions: **quantum wires**
- confinement in three dimensions: **quantum dots**

In quantum dots both electrons and holes can have only discrete energy values. Therefore, these systems are often denoted as **artificial atoms**. Compared to natural atoms the energy spectrum can be designed by changing the structure. The following figure 132 summarizes the different confinement regimes.

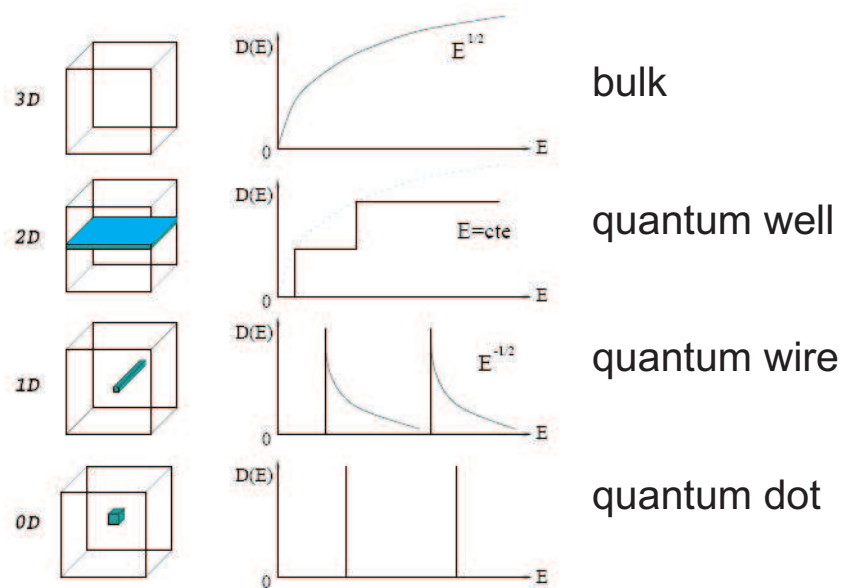


Figure 132: Different confinement regimes and density of states  $D(E)$  for electrons in bulk, quantum wells, quantum wires, and quantum dots.

While the bandgap influences the optical and electronic properties, for the growth of mono-crystalline heterostructures, the lattice mismatch  $(a_1 - a_2)/a_2$  between the substrate material (lattice constant  $a_1$ ) and the overgrown material ( $a_2$ ) becomes an important parameter. The growth of non-matched layers (e.g.  $a_1 = 0.605 \text{ nm}$  for InAs,  $a_2 = 0.565 \text{ nm}$  for GaAs,  $\Delta a/a = 7\%$ ) introduces a strain, whose energy accumulates with increasing layer thickness. When this energy exceeds certain critical levels, plastic relaxation occurs, such as the formation of misfit dislocations (figure 133), point defects, or islands (see subsection “Quantum Dots”).

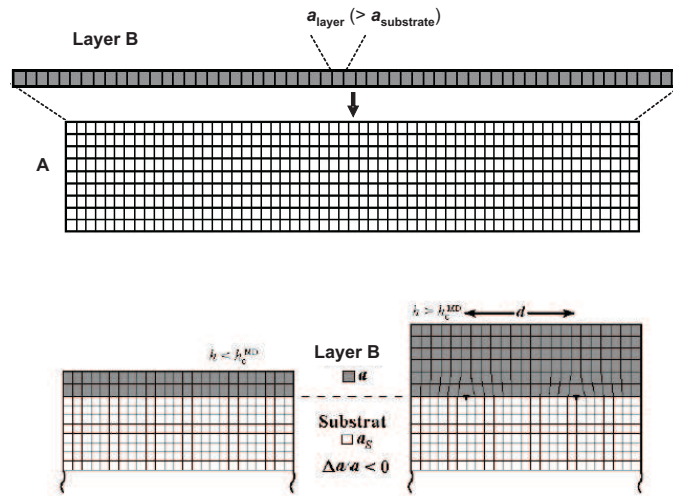
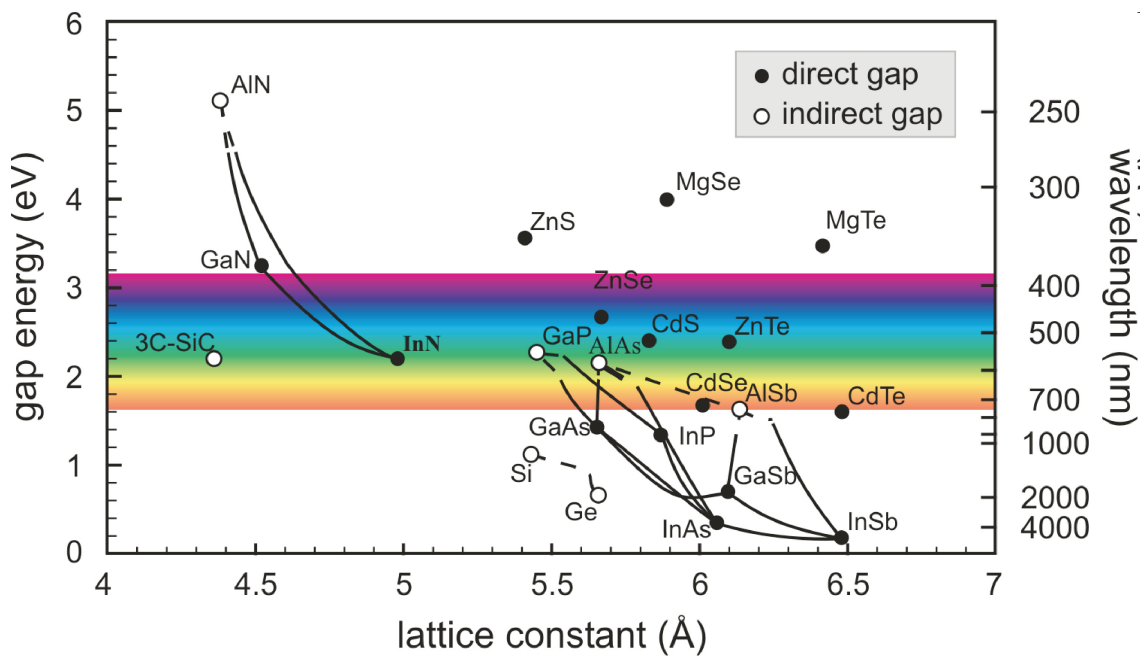


Figure 133: Growth of materials of different lattice constants; formation of misfit dislocations.

These defects often introduce additional, optically active energy levels. In order to avoid this, one has to remain below the critical thickness for defect formation and to properly choose the constituents according to their lattice mismatches (see figure 134).



[http://gorgia.no-ip.com/phd/html/thesis/phd\\_html/node4.html](http://gorgia.no-ip.com/phd/html/thesis/phd_html/node4.html)

Figure 134: Bandgap vs. lattice constant for various semiconductor materials.

Figure 135 shows an example of a defect-free GaAs–AlAs heterostructure. The combination GaAs–Al(Ga)As is of high interest in semiconductor optics, as the small lattice mismatch (0.28%) allows to grow large layers, while they have a comparably large difference in their refractive index (AlAs:  $n = 3.0$ ; GaAs:  $n = 3.6$  at  $\lambda = 900$  nm). This makes them ideal candidates for the formation of large monolithic Bragg reflectors.

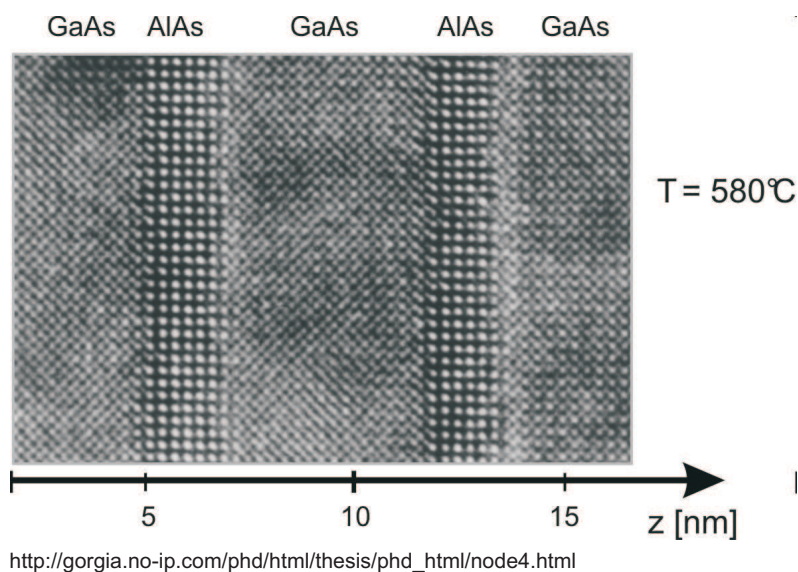


Figure 135: GaAs–AlAs super-lattice grown by MBE.  
 J. Lange, Resonante Tunnelstrukturen im System AlGaAs/InGaAs, master's thesis, University of Aachen RWTH, 1999.

### 5.3.2 Quantum Dots

Quantum dots (QDs) are particularly significant for optical applications due to their high quantum yield and discrete energy level structure. There are several approaches to use quantum dots as light-emitting diodes and as laser active material. In electronic applications they have been proven to operate like a single-electron transistor and show the Coulomb blockade effect. Quantum dots have also been suggested as implementations of qubits for quantum information processing, and as sources for single photon states.

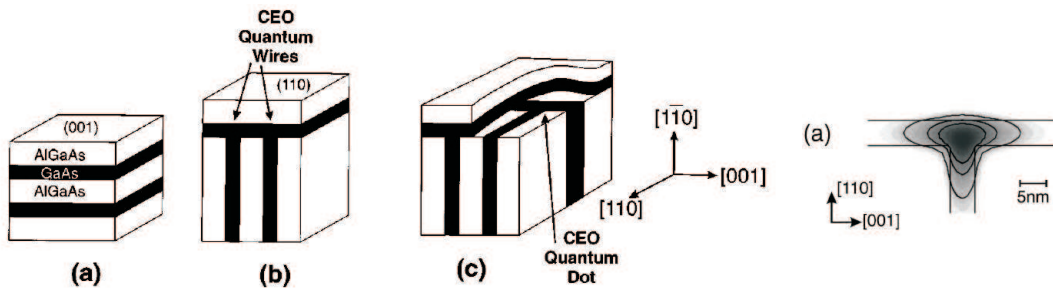


Figure 136: Quantum dots (and wires) form, e.g., in intersections of quantum wells. The sample is fabricated by cleaved edge overgrowth, where quantum wells are additionally grown on the sidewalls of the sample. Right: single-particle electron wave-function - the electron is trapped in the intersection forming a three-dimensional trapping potential. [from Grundmann and Bimberg, PRB 55, 4054 (1997)]

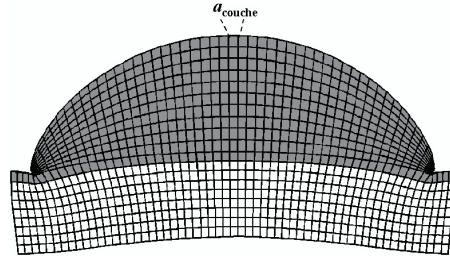
In contrast to the growth of 2-dimensional layers (quantum wells) the formation of quantum dots is less straightforward, as it requires the formation of small islands with sizes on the order of a few 10 nm.

#### Cleaved-edge overgrowth and natural quantum dots

In the past, QDs have been processed by starting from higher dimensional semiconductor heterostructures, like etching pillars in quantum well systems or forming intersections of quantum wells or quantum wires (figure 136). Also the growth of nano-structures on patterned substrates, such as grooves and pyramids led to successful quantum dot formation. So-called natural quantum dots are formed by width fluctuations mainly of quantum wells. In this environment the *excitons*, i.e., correlated electron-hole pairs, are trapped in broader regions of the quantum well, where the confinement energy is lowered, so that a potential minimum is formed.

### Self-assembled quantum dots

For epitaxially grown QDs, the most common technique exploits self-assembly of localized islands. Self-assembled QDs are formed when growing a semiconductor layer on top of a substrate material of smaller lattice constant. Above the critical thickness and under certain conditions, the strain relaxes by forming small islands, where at the surface the QD lattice constant relaxes to its bulk value (see figure 137).



H.T. Johnson and L.B. Freund,  
*J. Appl. Phys.* 81 (1997) 6081-6

Figure 137: Under certain conditions, strain in lattice-mismatched heterostructures relaxes to form islands, where at the surface the lattice constant of the added material relaxes to its bulk value.

This growth mode is called *Stranski-Krastanov growth*. Generally, a thin layer, which is known as the *wetting layer*, will remain, completely covering the substrate. The wetting layer forms a quantum well, which usually shows photoluminescence below the quantum dot emission wavelength. QDs are finally capped with (usually) the substrate semiconductor material to obtain a high quantum yield, i.e., avoiding non-radiative recombination via surface states.

As the emission properties of QDs do not only depend on the material, but also on size and shape, they can be used as optical emitters covering large spectral ranges from UV to IR. The InAs/GaAs system is by far the most studied of all QD systems, emitting in the infrared regime. InGaN quantum dots imbedded in GaN have the potential to cover the complete visible range. Finally II-VI systems such as CdSe/ZnSe or CdTe/ZnTe QDs luminesce in the 500-600 nm regime.

The following figures 138 and 139 show quantum dots in two different material systems (III-IV and II-VI materials):

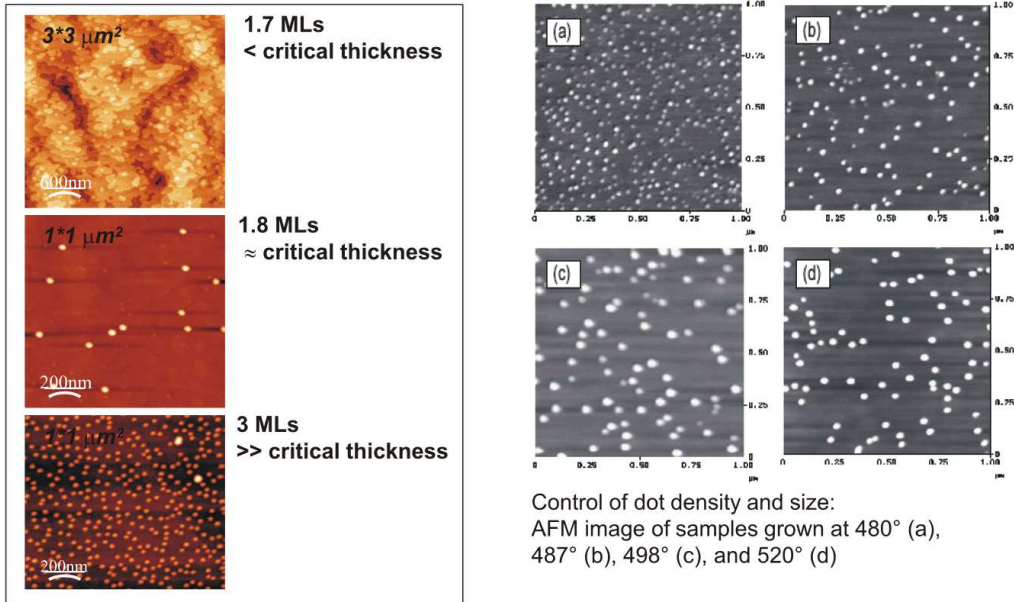


Figure 138: Left: Formation of quantum dots on a GaAs substrate while In deposition; Right: AFM images of quantum dots grown under different growth conditions

As pointed out quantum dots are a unique system as they are artificial light emitting objects with a discrete energy level structure. The following figure 140 shows a photoluminescence image of a sample containing approximately a dozen InP quantum dots, which are excited by a green laser. The spectrum of one of these dots is also displayed and shows the characteristic spectral lines.

Almost a continuous spectral regime from the UV to the near-infrared is accessible with quantum dot emitters grown by Stranski-Krastanow self-assembly as illustrated in figure 141.

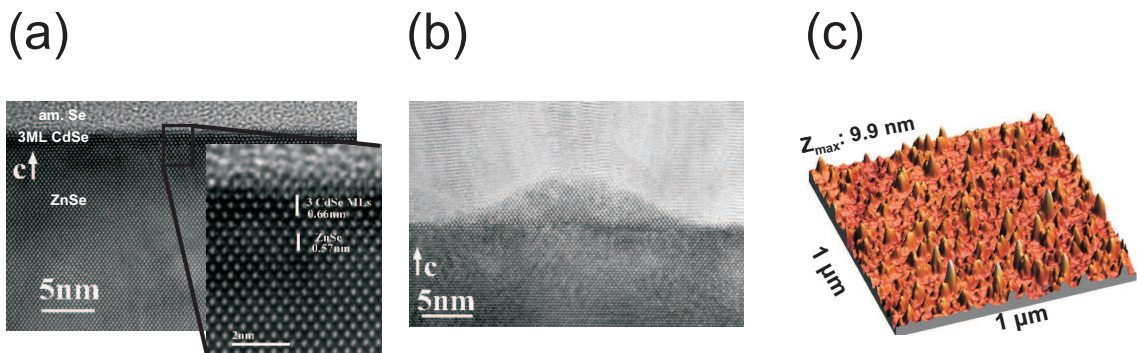


Figure 139: (a) TEM image of a CdSe layer on ZnSe below the critical thickness (3 ML). (b) Above the critical thickness it relaxes by forming a QD. (c) AFM image of CdSe QDs distributed on a ZnSe surface. [courtesy: CEA Grenoble, France]

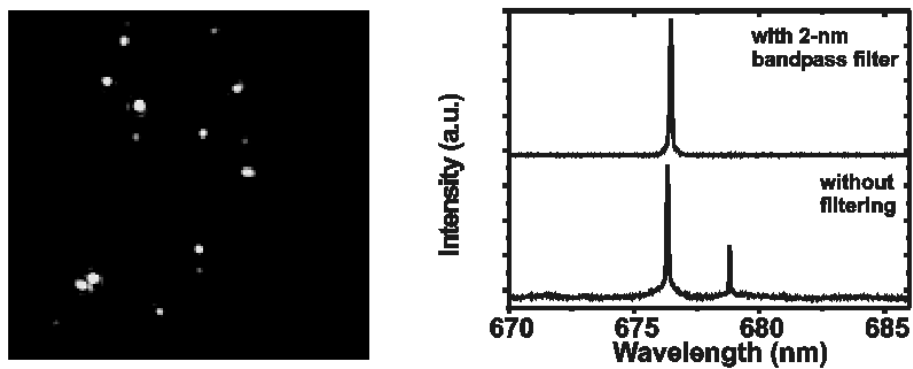


Figure 140: Left: Photoluminescence image of a sample containing several quantum dots (area approximately  $10 \mu\text{m} \times 10 \mu\text{m}$ ); Right: Discrete spectral lines from a single quantum dot.

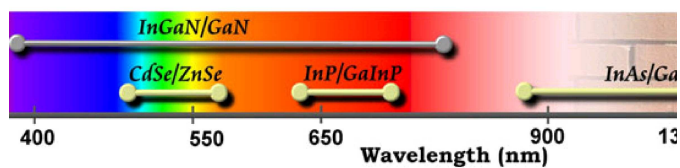


Figure 141: Schematic representation of the wavelength ranges accessible with different Stranski-Krastanow QD material systems.

### 5.3.3 Nanowires

In the past few years, the growth of nanowires (NWs) have found an increasing attention. These systems are semiconductors with ultra-high aspect ratios (length up to micrometers, and diameters even below 10 nm are possible). For inclusion of QD heterostructures they have the special advantage that strain relaxation can elastically happen on the narrow sidewalls, so that there are no restrictions to the sizes any more, which makes self-assembly obsolete. As a further consequence, there is no wetting layer, that otherwise can introduce non-radiative escape channels for the charge carriers out of the QD. For biological/medical analysis NW sample are interesting as sensors due to the huge surface-to-volume ratio.

One of the most frequently employed technique for epitaxial NW growth is the Vapour-Liquid-Solid (VLS) growth method. This process was originally developed by Wagner & Ellis in the 1960s to produce micrometer sized whiskers. Starting from 1990s, this technique was employed by many researches to form nanowires and nanorods from a rich variety of materials. In the VLS method, one starts with nanometer-sized metal particles, that are deposited on the surface. During the growth the substrate is heated above the melting point of the metal nanoparticles to a temperature at which it forms an eutectic phase with one of the epitaxial semiconductor reactants. The continued feeding of the semiconductor atoms into the liquid droplet supersaturates the eutectic. This alloy acts as a reservoir of reactants, which favours the growth at the solid-liquid interface and thus forms a one-dimensional nanowire with the alloy droplet remaining on the top. The size of the metal particle also affects the diameter of the nanowire and its growth speed.

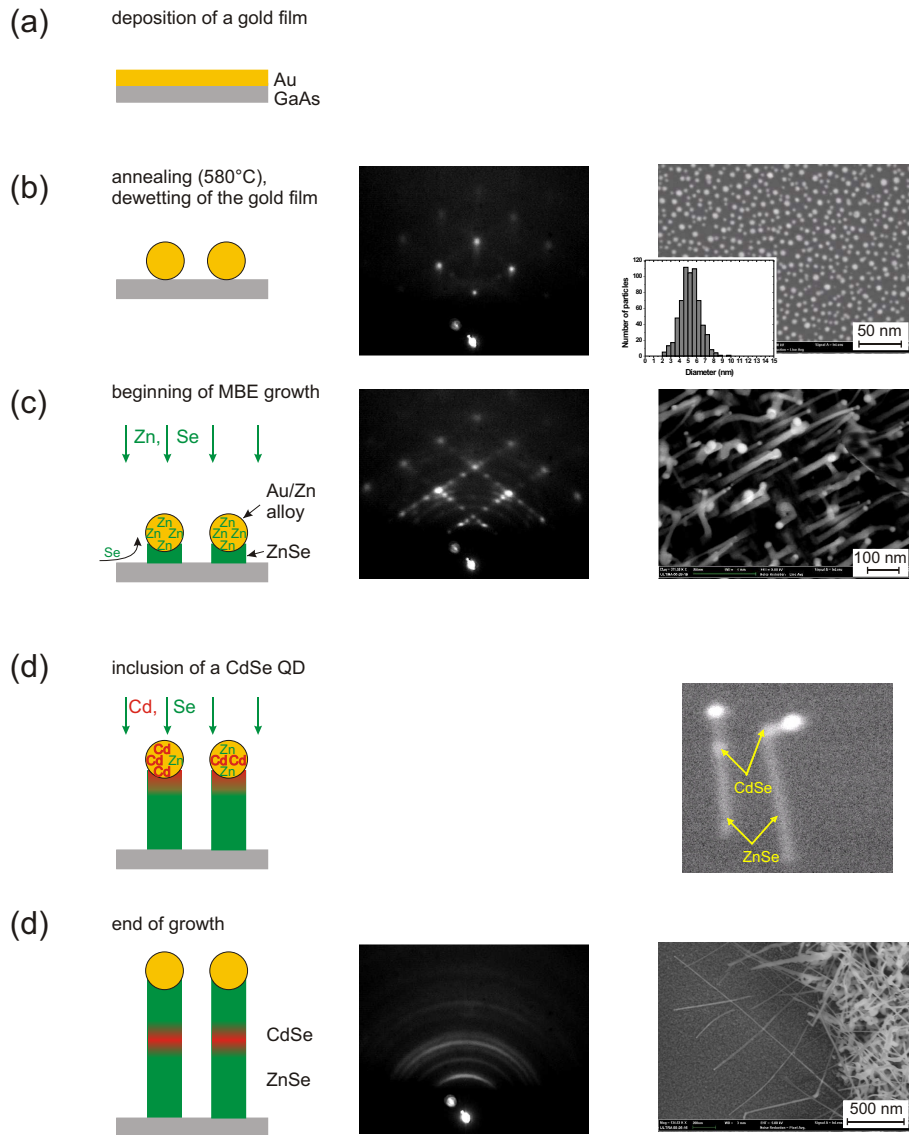


Figure 142: Principle of the VLS growth on the example of ZnSe MBE growth at 450°C. Left column: schematics of the growth. Central column: RHEED images obtained during growth. Right column: SEM images of the sample after the respective growth step. The inset in (b) shows the size distribution of the gold particles after annealing of a 0.5-nm film.

## 5.4 Chemical Synthesis

Semiconductor nanocrystals (NC) or colloidal QDs are small semiconductor crystallites which are made by organometallic chemical methods and are composed of a semiconductor core capped with a layer of organic molecules (Murray et al. 1993). The organic capping prevents uncontrolled growth and agglomeration of the nanoparticles. It also allows NCs to be chemically manipulated as if they were large molecules, with solubility and chemical reactivity determined by the identity of the organic molecules, figure 143. The capping also provides passivation of NCs; that is, it terminates dangling bonds that remain on the semiconductors surface. The unterminated dangling bonds can affect the NCs emission efficiency because they lead to a loss mechanism wherein electrons are rapidly trapped at the surface before they have a chance to emit a photon. Using colloidal chemical syntheses, one can prepare NC with nearly atomic precision; their diameters range from nanometers to tens of nanometers and size dispersions as narrow as 5%. Because of the quantum-size effect, this ability to tune the NC size translates into a means of controlling various NC properties, such as emission and absorption wavelengths.

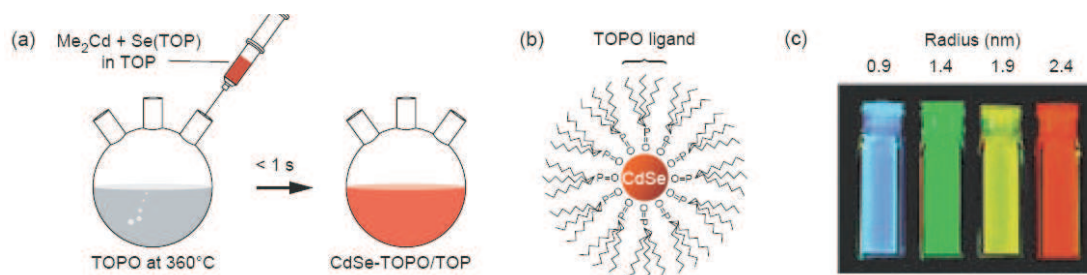


Figure 143: (a) An organometallic method is used for the fabrication of highly monodisperse CdSe NCs. Nucleation and subsequent growth of NCs occurs after a quick injection of metal and chalcogenide precursors into the hot, strongly coordinating solvents mixture of trioctylphosphine (TOP) and trioctylphosphine oxide (TOPO) in the case shown. After a fixed period, removing the heat source stops the reaction. As a result, NCs of a particular size form. (b) The colloidal NCs obtained by the method illustrated in (a) consist of an inorganic CdSe core capped with a layer of TOPO/TOP molecules. (c) Solutions of CdSe NCs of different radii, under ultraviolet illumination, emit different colours because of the quantum size effect. A 2.4-nm-radius dot has an energy gap of about 2 eV and emits in the orange, whereas a dot of radius 0.9 nm has a gap of about 2.7 eV and emits a blue colour. [from V.I.Klimov, *Los Alamos Science* 28, 214 (2003)]

There are three main effects that degrade the optical quality of nanoscopic emitters, such as molecules, quantum dots, or nanocrystals, in particular at room temperature:

### 1. photobleaching

Optical excitation provides energy to drive photo-chemical reactions. Often these reactions start from (higher) excited states and can lead to states which do not fluoresce or fluoresce with reduced quantum yield or at difference wavelength. Also changes of the matrix in the immediate neighboring environment of the emitters may influence the optical properties (e.g. charge traps).

### 2. blinking

The fluorescence intensity may fluctuate in an irregular way. This is a particular problem of nanocrystals as charges may be trapped at the surface (surface traps). The resulting electric fields radically reduce the radiative recombination rate and non-radiative processes dominate. After some time the charges are released and the emitter comes back to a fluorescing state.

The following figure 144 shows a simple three-level model to describe blinking and an observed intensity trace.

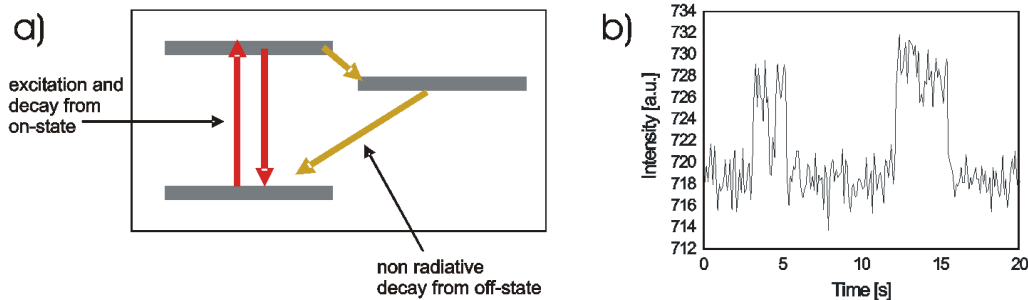


Figure 144: a) Simple three-level model for blinking; b) Measured intensity trace of a single nanocrystal.

### 3. spectral diffusion

Similar as described in the previous two points the state of the emitter or its immediate environment may be changed by optical excitation. This leads to blinking or to spectral jumps.

In the case of self-assembled quantum dots the large amount of free carriers which are created by above-band excitation leads to significant spectral diffusion. This typically limits the linewidth to above the Fourier-limit. Nearly resonant excitation can be used to reduce this effect. Also after different warming-up and cooling-down cycles the emission wavelength may change.

Colloidal NCs with variable surface chemistry are ideal building blocks for creation of different superstructures, like composite polymer/nanocrystal films, composite core-shell microspheres, 1D, 2D and 3D NC arrays. An example of a crystal of nanocrystals is shown in figure 145.

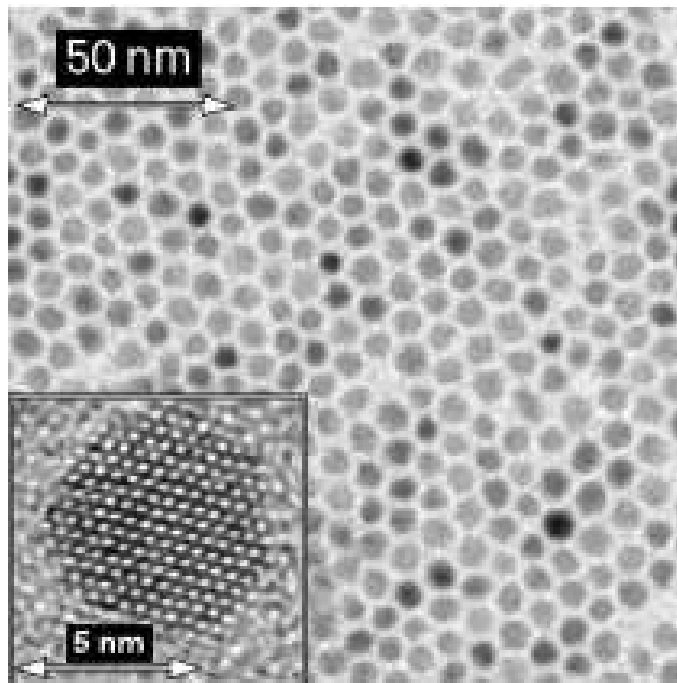


Figure 145: TEM image of an individual nanocrystal (inset) and an array of nanocrystals. [courtesy: A. Rogach, Munich]

Advanced optical spectroscopy studies on NCs and their superstructures address energy transfer, charge separation, and single particle luminescence. Highly luminescent semiconductor NCs are interesting for different applications, ranging from solar cells to biological fluorescent labels.

## 5.5 Lithography

The fabrication of structures (circuits) on a wafer requires a process by which specific patterns of various materials can be deposited on or removed from the wafer's surface. The process of defining these patterns on the wafer is known as *lithography*. Lithography uses photoresist materials to cover areas on the wafer that will not be subjected to material deposition or removal. (For more details of particularly silicon fabrication techniques see also [www.sliconfastread.com](http://www.sliconfastread.com).)

The following figure 146 illustrates the present state and limits of lithography technology.

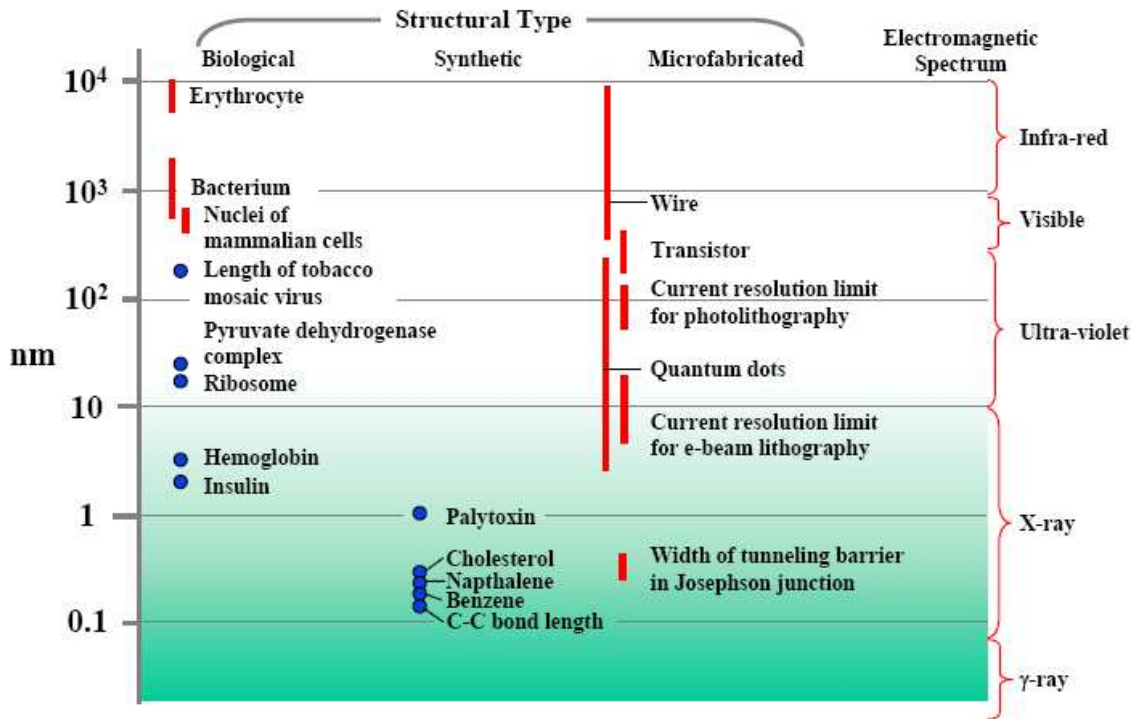


Figure 146: Overview of length scales and present limits of lithography technology [After Whitesides et al. Science, 2541312 (1992)]

### 5.5.1 Optical lithography

Optical Lithography refers to a lithographic process that uses visible or ultraviolet light to form patterns on the photoresist through printing. Printing is the process of projecting the image of the patterns onto the wafer surface using a light source and a photo mask.

Patterned masks, usually composed of glass or chromium, are used during printing to cover areas of the photoresist layer that shouldn't get exposed to light. Development of the photoresist in a developer solution after its exposure to light produces a resist pattern on the wafer, which defines which areas of the wafer are exposed for material deposition or removal.

There are two types of photoresist material, namely, negative and positive photoresist. Negative resists are those that become less soluble in the developer solution when exposed to light, forming negative images of the mask patterns on the wafer. On the other hand, positive resists are those that become more soluble in the developer when exposed to light, forming positive images of the mask patterns on the wafer.

In lithography, there are three types of printing which are introduced in the following:

- **Contact printing** refers to the light exposure process wherein the photomask is pressed against the resist-covered wafer with a certain degree of pressure. Contact printing is capable of attaining resolutions of less than 1 micron (0.25 micron or better). However, the presence of contact between the mask and the resist somewhat diminishes the uniformity of attainable resolution across the wafer. To alleviate this problem, masks used in contact printing must be thin and flexible to allow better contact over the whole wafer.

Contact printing also results in defects in both the masks used and the wafers, necessitating the regular disposal of masks (whether thick or thin) after a certain level of use.

- **Proximity printing** involves no contact between the mask and the wafer, which is why masks used with this technique have longer useful lives than those used in contact printing. During proximity printing, the mask is usually only 20-50 microns away from the wafer (see figure 147).

The resolution achieved by proximity printing is not as good as that of contact printing due to *Fresnel (or near-field) diffraction* of light resulting from the small gap between the mask and the wafer. Proximity printing resolution may be improved by diminishing this gap and by using light of shorter wavelengths.

- **Projection printing** involves no contact between the mask and the wafer. It employs a large gap between the mask and the wafer (see figure 147). Here, *Fraunhofer (far-field) diffraction* determines the resolution.

Projection printing is the technique employed by most modern optical lithography equipment. The resolution achieved by projection printers depends on the wavelength and coherence of the incident light and the NA of the lens. Using a lens with a higher NA will result in better resolution, but a decrease in the depth of focus of the system. Poor depth of focus will cause some points of the wafer to be out of focus, since no wafer surface is perfectly flat. Thus, proper design of any aligner used in projection printing considers the compromise between resolution and depth of focus.

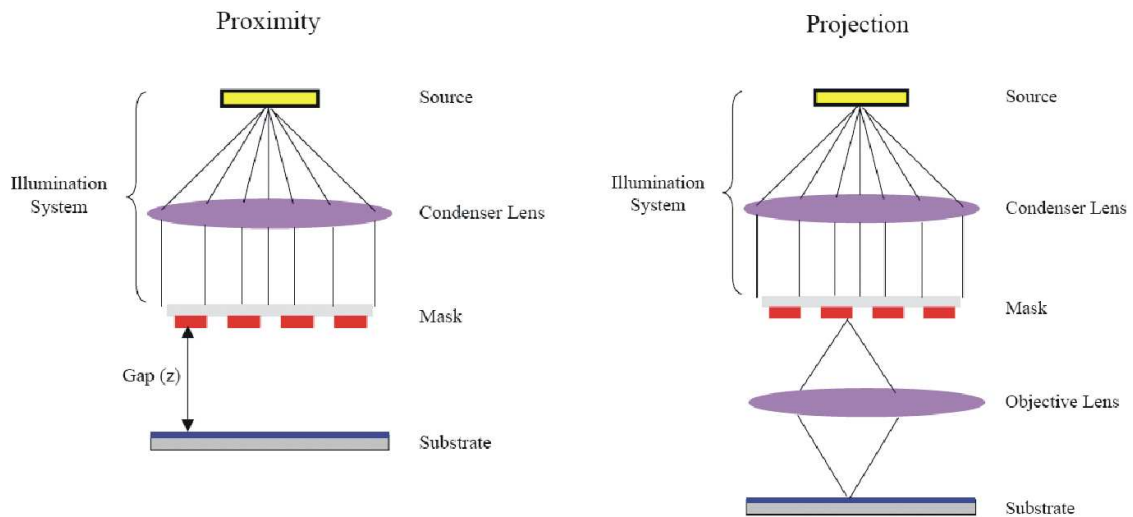


Figure 147: Schematics of proximity (left) and projection (right) printing. [from Anderson and Liddle, <http://e298a-ee290b.lbl.gov/>]

Optical lithography is finally limited by the wavelength used for excitation of the photoresist. The following figure 151 illustrates the present state of the art.

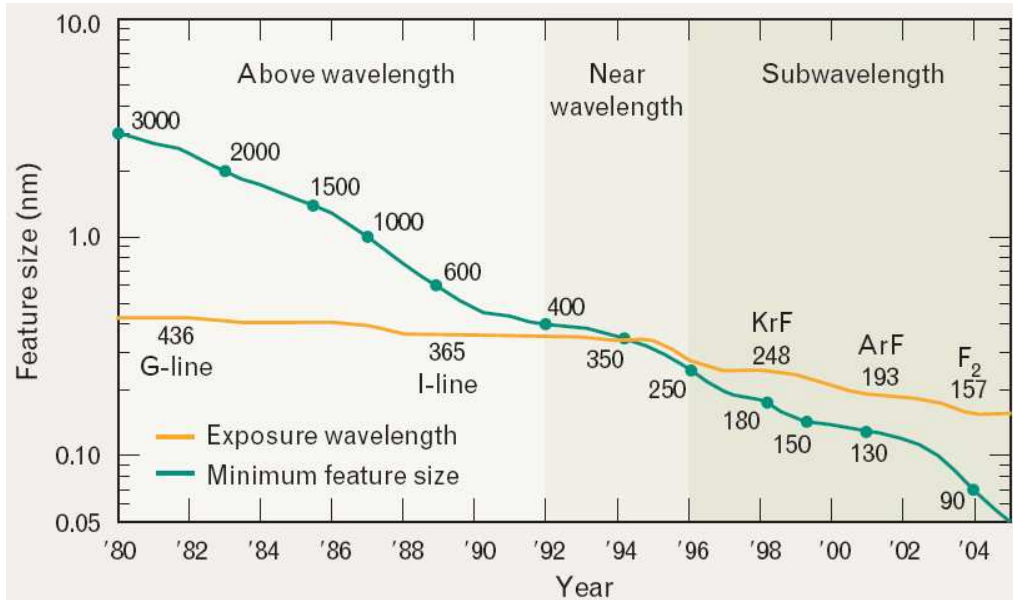


Figure 148: Reduction in minimum feature size and exposure wavelength over time. Mercury arc lamps produce the G-line at 436 nm and the I-line at 365 nm. The krypton-fluoride (KrF) excimer laser operates at 248 nm, the argon-fluoride (ArF) laser operates at 193 nm, and the fluorine (F<sub>2</sub>) excimer laser operates at 157 nm. [from M. Rothschild et al., Lincoln Lab. Journal, Vol. 14, No. 2, (2003)]

### 5.5.2 Electron-beam lithography

Electron Beam Lithography (e-beam lithography or EBL) refers to a lithographic process that uses a focused beam of electrons to form the circuit patterns needed for material deposition on (or removal from) the wafer, in contrast with optical lithography which uses light. Electron lithography offers higher patterning resolution than optical lithography because of the shorter wavelength possessed by the 10-50 keV electrons that it employs.

Given the availability of technology that allows a small-diameter focused beam of electrons to be scanned over a surface, an EBL system doesn't need masks anymore to perform its task. An EBL system simply 'draws' the pattern over the resist wafer

using the electron beam as its drawing pen. Thus, EBL systems produce the resist pattern in a 'serial' manner, making it slow compared to optical systems.

The following figure 149 shows the major components of an e-beam system:

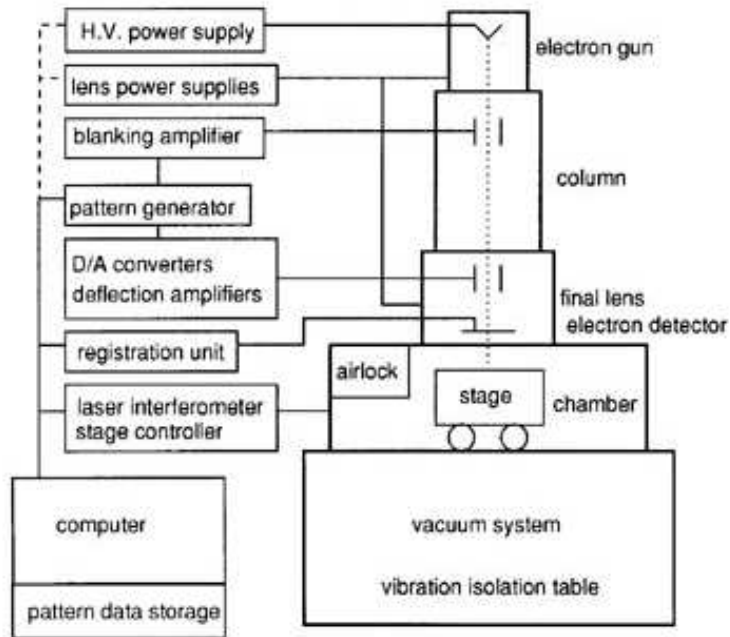


Figure 149: Block diagram showing the major components of a typical electron beam lithography system [from SPIE Handbook of Microlithography, Micromachining and Microfabrication]

A typical EBL system consists of the following parts:

- an *electron gun or electron source* that supplies the electrons
- an *electron optics* that 'shapes' and focuses the electron beam
- a *mechanical scanning stage* that positions the wafer under the electron beam
- a *wafer handling system* that automatically feeds wafers to the system and unloads them after processing
- a *computer system* that controls the equipment

Just like optical lithography, electron lithography also uses positive and negative resists, which in this case are referred to as electron beam resists (or e-beam resists). E-beam resists are e-beam-sensitive materials that are used to cover the wafer according to the defined pattern. A common resist is polymethyl methacrylate (PMMA).

The resolution of optical lithography is theoretically limited by diffraction (wavelength of the electrons on the order of 0.2-0.5 angstroms). However, main constraints are due to the following effects:

- **electron scattering**

During electron beam lithography, scattering occurs as the electron beam interacts with the resist and substrate atoms (see figure 150). Scattering broadens the diameter of the incident electron beam and gives the resist unintended extra doses of electron exposure. Both effects result in wider images than what can be ideally produced from the e-beam diameter. In fact, closely-spaced adjacent lines can 'add' electron exposure to each other, a phenomenon known as *'proximity effect'*.

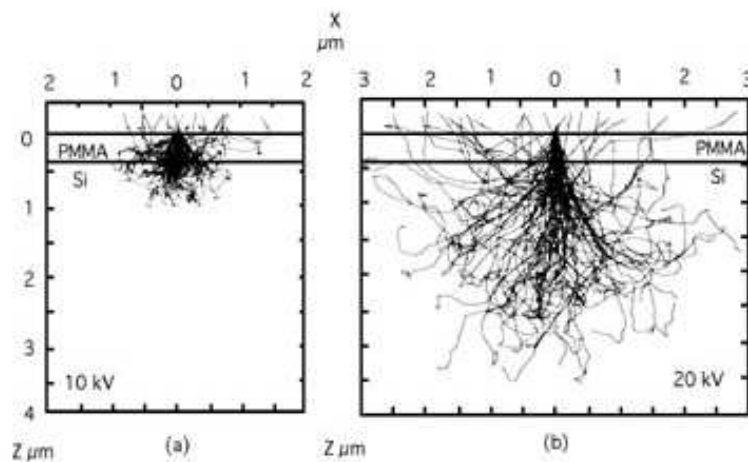


Figure 150: Monte Carlo simulation of electron scattering in resist on a silicon substrate at a) 10 kV and b) 20 kV. [From Kyser and Viswanathan, J. Vac. Sci. Technol. 12, 1305-1308 (1975)]

- **resist swelling**

Resist swelling occurs as the developer penetrates the resist material. The resulting increase in volume can distort the pattern, to the point that some adjacent lines that are not supposed to touch become in contact with each other.

- **aberrations**

Compared to optical systems electron beam optics suffers from enhanced aberrations. As in optics this increases the size of the smallest available spot and thus the resolution.

The last figure 151 of this section provide an example of complex integrated circuits written by electron beam lithography.

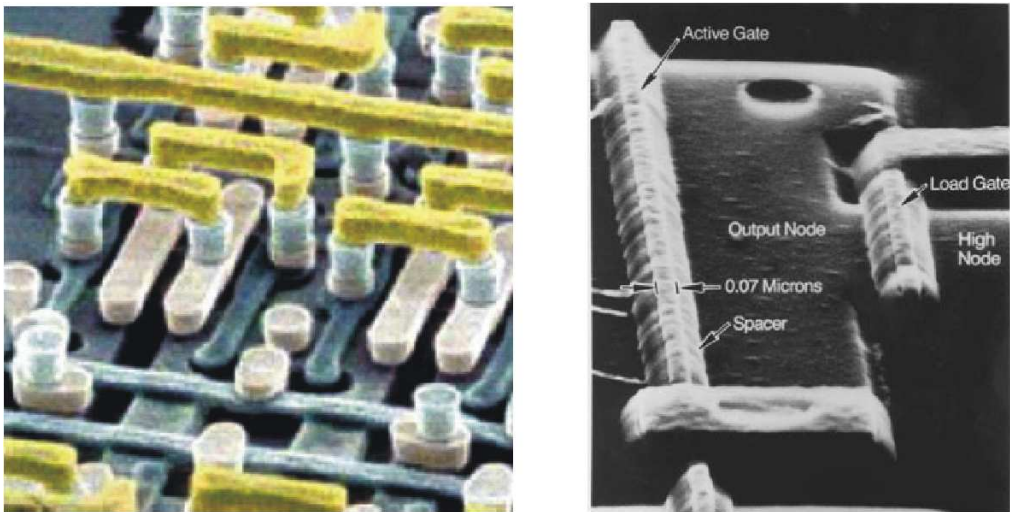


Figure 151: Examples of two complex structures written by e-beam lithography. [from IBM]